Proceedings of the 14th IASTED International Conference
Robotics and Applications (RA 2009)
November 2 - 4, 2009 Cambridge, MA, USA

WORKSPACE OPTIMIZATION OF THE ROBOCOASTER USED AS A MOTION SIMULATOR

Simon Schaetzle, Carsten Preusche and Gerd Hirzinger
Institute of Robotics and Mechatronics
German Aerospace Center (DLR)
D-82234 Wessling, Germanny
email: Simon.Schaetzle@dlr.de

ABSTRACT
The RoboCoaster is a theme park ride based on a serial chain industrial robot. Apart from its use as an entertainment device it can also be used for motion simulation such as flight or driving simulation. Its joint angle ranges are strictly limited due to safety reasons. In order to provide an appropriate workspace for motion simulation it is necessary to redefine the hardware limits of each joint. In this paper, we discuss the optimization of the robot's joint angle ranges and present a method to reduce the six-dimensional optimization problem to a two-dimensional one. This method is illustrated using the example of a driving and flight simulator. We managed to expand the workspace significantly and to enhance the range of translational movements by a factor of up to five.

KEY WORDS
Flight simulator, Robot design and architecture, RoboCoaster, Workspace optimization, Joint angle limitation, Joint angle ranges

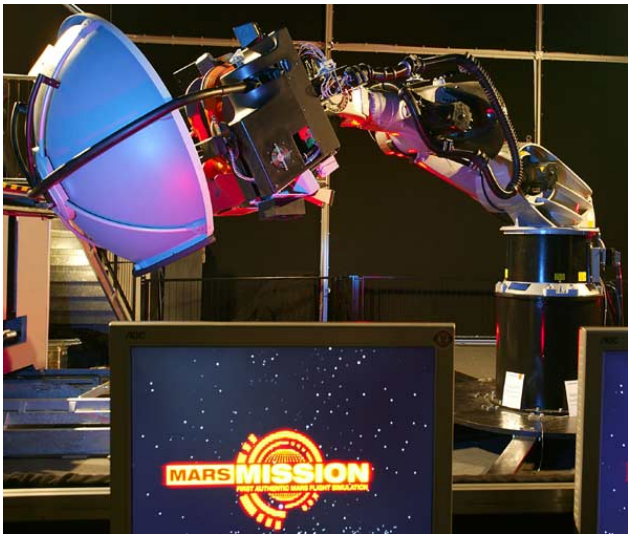

Figure 1. RoboCoaster used as a motion simulator

1 Introduction

Most of the existing motion simulators are based on a six degree of freedom (DoF) hexapod-kinematic structure (D. Stewart [1]). These systems are able to move large weights while they are rather strongly restricted in their size of workspace and movement capability. Maneuvers for example such as skidding in a car ride or rolling of a plane are difficult to realize with such platforms as realizable tilt angles are quite small.

Current research investigates the use of a serial chain industrial robot as a motion simulator [2],[3]. This idea is based on the RoboCoaster [4] presented by KUKA robotics in the year 2002. The RoboCoaster is a modified KUKA KR500 industrial robot [5] with a roller coaster seat mounted to its tool flange. This innovative concept enables for example spectacular theme park rides with spectacular loops.

Apart from the use as an entertainment device the RoboCoaster can be used for motion simulation [6]. Low acquisition cost and a rather big workspace make the RoboCoaster a promising alternative to conventional motion simulators. Using appropriate motion cueing [7],[8] and path planning [9], it can be used for a wide spectrum of applications [10].

Depending on the application, different constraints with respect to the workspace exist. In flight simulations, the pilot should be able to roll (rotation axis rectangular to the backrest) whereas in drive simulations a horizontal translation is important to imitate evasive or overtaking manoeuvers [11].

The RoboCoaster's joint angle ranges are strictly limited due to safety reasons. In this way it is guaranteed that the passenger can not collide e.g. with the floor or the robot itself. However, this issue causes a severe restriction of the robot's workspace. In addition to the limitation by software, mechanical buffers in each joint restrict the joint angle ranges. In case of a crash into the joint angle limits due to an error (e.g. technical fault or program error), these deformable mechanical buffers absorb kinetic energy safeguarding the human from getting injured by an extremely high deceleration.

Comparing the workspaces of a RoboCoaster and a KR500 (with mounted seat) one notices that the spherical shell of the RoboCoaster is much thinner than that of the KR500 (see figure 2). Reachable positions of the Robo-

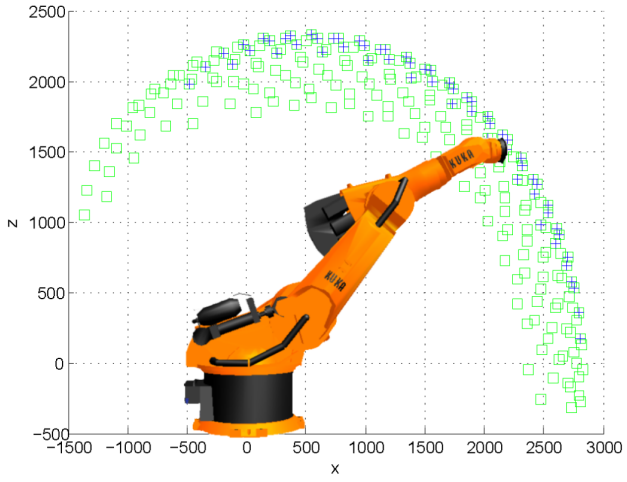

Figure 2. Sectional drawing of the workspaces of a RoboCoaster (plus signs) and a KR500 (rectangles) at $q1 = 0$

Coaster are marked with small plus signs and with small rectangles for the KR500. The limited workspace of the RoboCoaster is well suited to spectacular rides including loops. However it is not suited for drive and flight simulations as translational movements are very limited in all directions. In order to provide an appropriate workspace for motion simulation it is necessary to optimize the workspace by redefining the mechanical buffers' positions of each joint.

2 Formulation of optimization problem

In order to use the RoboCoaster in the best way as a motion simulator, the hardware limits of each joint have to be optimized. Depending on the application of the simulator, different constraints concerning the workspace are specified. For example, long lateral movements are required to imitate an overtaking maneuver whereas large rotations are necessary to roll the pilot. There is a strong dependency among the joint angles. The limitation of one joint has an effect on other joints. Therefore an independent maximization of every single joint angle range is impossible.

Consequently the following optimization problem with the listed side conditions can be formulated:

$$\max_{\vec{q} \in R^6} \ \vec{\omega} \cdot \vec{f}_{kin}(\vec{q}) \qquad (1)$$

with

$$\vec{f}_{kin}(\vec{q}) = \{\Delta x, \Delta y, \Delta z, \Delta\alpha, \Delta\beta, \Delta\gamma\}^T$$

and $(x, y, z) \mathrel{\widehat{=}}$ cartesian position, $(\alpha, \beta, \gamma) \mathrel{\widehat{=}}$ yaw, pitch, roll rotation angle as well as the weighting factor vector $\vec{\omega} \in R^6$. There are three kinds of side conditions:

- Joint angle limitations from hardware
  SC1:

$$\vec{q} \in]\vec{q}_{min},\ \vec{q}_{max}[$$

- No collision
  SC2:

$$V(object_i, \vec{q}) \quad \cap \quad V(object_k, \vec{q}) = \emptyset$$

  with $object_i = \{passengercabin, robot, \ldots\}$ and $object_k = \{robot, floor, pedestal, \ldots\}$

- Joint angle limits and requirements from application
  SC3:

$$\begin{aligned} \vec{f}_{kin}(\vec{q}) &\in]\vec{c}_{i,min},\ \vec{c}_{i,max}[\\ \vec{f}_{kin}(\vec{q}) &> \vec{c}_i \\ \vec{q} &\in]\vec{q_c}_{min},\ \vec{q_c}_{max}[\\ \vec{q} &> \vec{q_c} \\ \vec{c}_i, \vec{q_c} &\in R^6 \end{aligned}$$

These three kinds of side conditions are discussed below.

2.1 Side condition: joint angle limitations from hardware

The robot's valid joint angle ranges are specified by the manufacturer in a technical data sheet. Typically there are software and hardware joint limitations and software limits are within the hardware limits.

2.2 Side condition: no collision

The design of the passenger cabin has a significant effect on the definition of joint angle ranges. The following parameters are of interest: dimension of passenger cabin, flange position and flange angle, enveloping volume of passenger cabin including reachable positions by the passenger's limbs.

It must be guaranteed during the whole motion simulation that collisions cannot occur. The collision detection checks for collisions between passenger cabin and robot, pedestal, floor and entry area as well as collisions between robot and pedestal and entry area. The volume of one object may not have overlapping sections with any other object:

$$V(object_i, \vec{q}) \quad \cap \quad V(object_k, \vec{q}) = \emptyset$$

with $object_i = \{passenger\ \ cabin, robot, \ldots\}$ and $object_k = \{robot, floor, pedestal, \ldots\}$

2.3 Side condition: joint angle limits and requirements from application

Depending on the application of the simulation, different constraints of joint angles and requirements concerning the workspace must be fulfilled. For instance lateral movements without change of the passenger cabin's orientation can be required that implies joint angle limits of

$q4 >= |90\ °|$ (see 4.4). Side conditions of absolute minimum and maximum values (e.g. q_{min}, q_{max}) and side conditions of relative values (e.g. $\Delta y > 1m$) are derived:

$$\begin{aligned} \vec{f}_{kin}(\vec{q}) &\in]\vec{c}_{i,min},\ \vec{c}_{i,max}[\\ \vec{f}_{kin}(\vec{q}) &> \vec{c}_i \\ \vec{q} &\in]\vec{q}_{cmin},\ \vec{q}_{cmax}[\\ \vec{q} &> \vec{q}_c \\ \vec{c}_i, \vec{q}_c &\in R^6 \end{aligned}$$

3 Optimization - approach

If the dimensions of the passenger cabin are known, an enveloping volume of the passenger cabin including reachable positions by the passenger's limbs can be generated. Next, a collision detection for all possible combinations of joint angles is performed. The collision detection checks for collisions between passenger cabin and robot, pedestal, floor and entry area as well as collisions between robot and pedestal and entry area. The results of this collision check with user-defined resolution are stored in a database.

Considering specific constraints of joint angles and requirements with respect to the workspace, ranges of joint angles $q4$, $q5$ and $q6$ are specified as side conditions for the optimization problem (see SC3 in 2.3). These joint angle ranges have a strong influence on the workspace and the definition of joint angle ranges $\vec{q2}$ and $\vec{q3}$ (with $\vec{q_i} = (q_{i_{min}}, q_{i_{max}})$. An example of the KR500 joint axis and their sense of direction is shown in figure 3. If

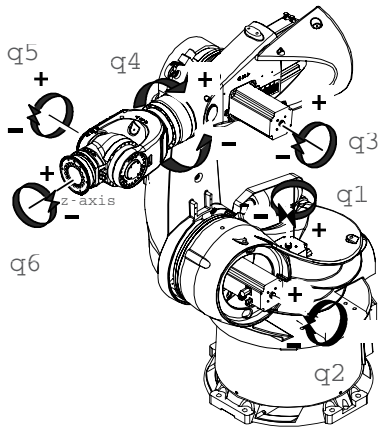

Figure 3. Joint axis of KR500 and their sense of direction. Current configuration: $q1 = 0°, q2 = -90°, q3 = 90°, q4 = 0°, q5 = 0°, q6 = 0°$

these joint angle ranges are specified first, the complexity of the workspace optimization can be reduced from a six-dimensional to a two-dimensional optimization problem, that is the optimization of $\vec{q2}$ and $\vec{q3}$. Therefore, a configuration space of joints two and three is necessary. It can be generated on the basis of the collision check's results which were stored earlier.

The configuration space indicates valid joint angle combinations of $q2$ and $q3$. For each combination of $q2$ and $q3$, angles $q4$, $q5$ and $q6$ are varied within previously specified ranges of angle. If any collision occurs in one of these possible joint angle combinations, the appropriate $q2$, $q3$ combination is marked with a red circle otherwise it is marked with a blue asterisk (no collision).

An exemplary configuration space is shown in figure 4. The axis of abscissa shows joint angle $q2$, the axis of ordinates shows $q3$.

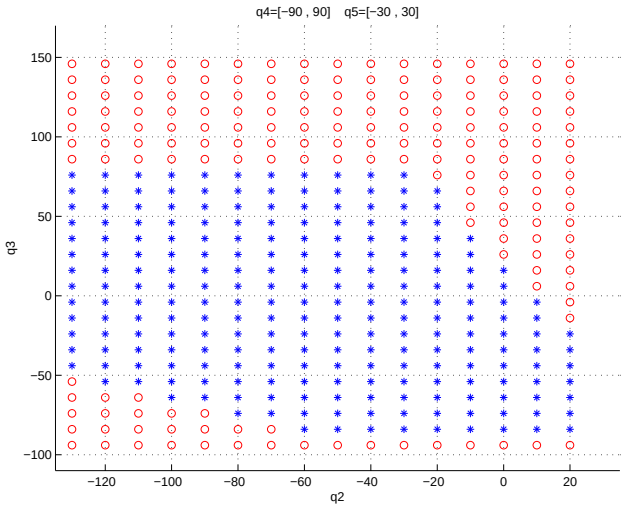

Figure 4. Example of a configuration space of joints two and three

The generation and the use of configuration spaces allows to reduce the six-dimensional optimization problem (see equation 1) to a two-dimensional one:

$$\max_{\vec{q} \in R^2} A(\vec{q}) \tag{2}$$

with rectangular area

$$A(\vec{q}) = (q2_{max} - q2_{min}) * (q3_{max} - q3_{min})$$

and $A(\vec{q}) \in S, S \mathrel{\widehat{=}}$ crowd of combinations of joint angles q2 and q3 without collisions. Due to the design of the robot, joint angle $q1$ has no influence on the optimization problem as it is assumed that there is no additional obstacle within the rotationally-symmetric workspace of the robot.

4 Example - driving and flight simulator

In the following example the RoboCoaster is modified for the use as a driving and flight simulator. The passenger cabin must be able to perform long translational (overtaking maneuver) and large rotational (roll maneuver of the pilot) movements. The presented optimization approach is applied to this case study. The robot's joint axis and their sense of direction is depicted in figure 3.

4.1 Passenger cabin

The passenger cabin consists of two seats and a hood with integrated screens and ventilation for a better immersion into the scenario. The cabin is mounted to the tool flange of the robot in a way that the backrest is orientated at right angles to the tool flange. This enables to roll the pilot with little joint activity (only axis six must rotate). The envelop-

Figure 5. Enveloping rotationally-symmetrical volume, mounted to the robot's tool flange

ing volume of the cabin is assumed to be a rotationally symmetrical geometry around the z-axis of the sixth joint for the upcoming collision detection (see figure 5). This volume and its radii are based on the dimensions of the cabin and the positions that are reachable by the limbs of a human of $1,90m$ size. The cabin and its dimensions are depicted in figure 6. A volume of corresponding size is created with the help of a computer-aided-design software. The collision detection is performed afterwards.

4.2 Joint angle limitation from hardware

Hardware and software joint limits are listed in the data sheet of the RoboCoaster [4] and the KR500 [5]. Software limits are within the hardware limits.

4.3 Collision detection

Within a suitable simulation software, the generated volume is attached to the robot's tool flange. All possible combinations of joint angles $q2$, $q3$, $q4$ and $q5$ are checked for collisions with a resolution of $10°$. Collision check results are stored in a database. Joint angle $q1$ has no influence on the collision check as it is assumed that there is no additional obstacle within the robot's rotationally-symmetric workspace around axis one. The collision detection checks for collisions between passenger cabin and robot, pedestal (height $1,05m$), floor and entry area as well as collisions between robot and pedestal and entry area.

Due to the rotationally-symmetrical volume mounted to the flange, joint angle $q6$ has no influence on this investigation and collision detection results are ignored for $q6$. It

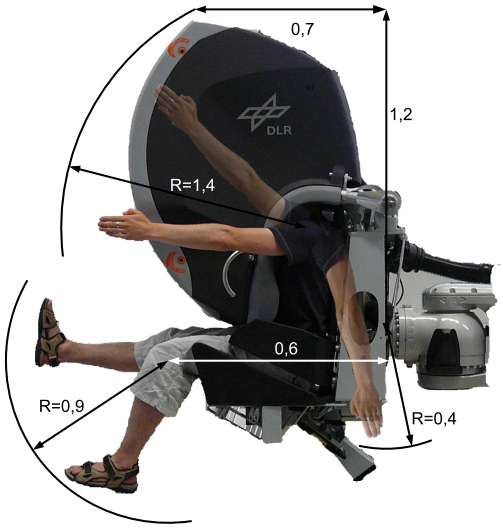

Figure 6. Passenger cabin and its dimensions in meters

is advantageous to check all possible combinations of joint angles at first and to investigate desired joint angle combinations in a second step. The time consuming collision detection is then executed only once.

Once the desired joint angle ranges $\vec{q4}$ and $\vec{q5}$ are defined, the configuration space of $q2$ and $q3$ can be generated quickly. Joint angle range $\vec{q6}$ is unchanged in comparison to the industrial robot KR500 as the rolling of the passenger cabin shall be enabled. Joint angle $q2$ and $q3$ vary within the maximum joint angle limits of the KR500 whereas ranges $\vec{q4}$ and $\vec{q5}$ are determined in 4.4).

4.4 Joint angle limits and requirements from application

The joint angle ranges $\vec{q4}$ and $\vec{q5}$ have a strong influence on the workspace and the optimization of the ranges $\vec{q2}$ and $\vec{q3}$. If these joint angle ranges are specified first, the complexity of the workspace optimization can be reduced from a six-dimensional to a two-dimensional optimization problem (that is the optimization of $\vec{q2}$ and $\vec{q3}$).

There are no constraints on joint angle $q1$ as this joint has no influence on the configuration space.

Joint angle $q3$ is crucial for the elbow orientation of the robot. If the sign of $q3$ switches, the configuration of the elbow (up/down) changes. A six axis robot cannot change elbow orientation without change of pose. In most cases of motion simulations this change of configuration is disturbing and has to be avoided. Therefore, this side condition is formulated: $q3_{min} > 0°$.

Driving simulations often require lateral movements. Due to the robot's kinematic structure and movement capability, a constraint of joint angle $q4$ must be $q4_{max} \geq 90°$ and $q4_{min} \leq -90°$, if the passenger cabin's orientation shall stay constant while moving sideways and if it is mounted at the backrest as described in this example.

There are two constraints of joint angle $q5$. First, $q5$ must be limited to $q5 \in [-65°, 65°]$ otherwise the passenger cabin and the robot can collide. Second, $q5$ must be $q5_{min} > 30°$ to avoid a singularity in joint five.

Joint angle range $\vec{q6}$ is not limited ($q6 \in [-350°, 350°]$), as the rolling of the passenger cabin is easy to realize with a rotation in joint six.

4.5 Configuration space

The following figures show configurations spaces of different $q5$ ranges. Ranges from $q5 \in [-35°, 35°]$ to $q5 \in [-65°, 65°]$ are investigated with a resolution of $10°$.

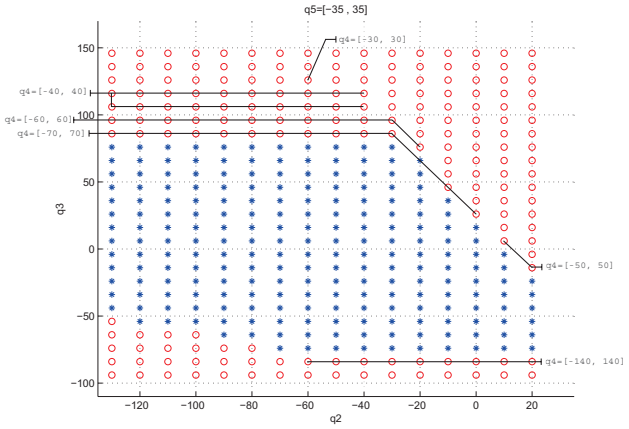

Figure 7. Configuration space at $q5 \in [-35°, 35°]$, $q4 \in [-350°, 350°]$ and $q6 \in [-350°, 350°]$

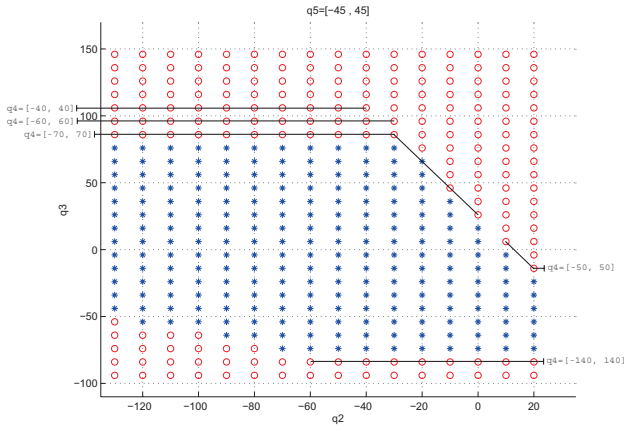

Figure 8. Configuration space at $q5 \in [-45°, 45°]$, $q4 \in [-350°, 350°]$ and $q6 \in [-350°, 350°]$

Combinations of $q2$ and $q3$ without collisions are marked with blue asterisks and are valid for all ranges of $q4$ ($q4 \in [-10°, 10°]$ to $q4 \in [-350°, 350°]$). Plotted lines expand the collision-free area for ranges of $q4$ that are smaller than the ranges indicated beside these lines. For example, in figure 8 the collision-free area is expanded at $q3 = 86°$ and $q2 \in [-130°, -30°]$, if $q4 \leq |70°|$.

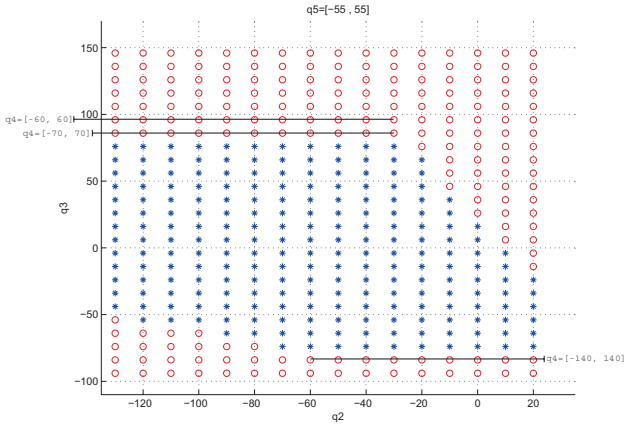

Figure 9. Configuration space at $q5 \in [-55°, 55°]$, $q4 \in [-350°, 350°]$ and $q6 \in [-350°, 350°]$

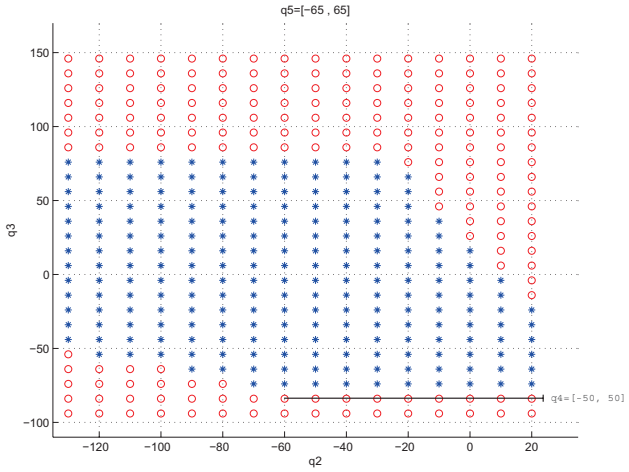

Figure 10. Configuration space at $q5 \in [-65°, 65°]$, $q4 \in [-350°, 350°]$ and $q6 \in [-350°, 350°]$

The effect of varying joint angle ranges on the workspace is well visible in the different configuration spaces that are shown below. If compared, one notice that

- there is an area without collisions which is identical for all $q5$ ranges ($q5 \in [-35°, 35°]$ to $q5 \in [-65°, 65°]$) and which is valid for all $q4$ ranges
- the collision-free area is only expanded if joint angle $q4 \in [-70°, 70°]$. One exception is at $q3 = -84°$, $q2 \in [-60°, 20°]$ and $q4 \in [-140°, 140°]$)

- the bigger the joint angle range $\vec{q5}$ the smaller the influence of $\vec{q4}$ on the area without collisions.

According to these findings, two conclusions can be drawn:

- conclusion 1: as the influence of $\vec{q4}$ occurs only if $q4 \in [-70°, 70°]$ and the requirement $q4_{max} \geq 90°$ and $q4_{min} \leq -90°$ is above this threshold, $\vec{q4}$ can be specified without limitation: $q4 \in [-350°, 350°]$
- conclusion 2: if $\vec{q4}$ is specified as a range $q4 \in [-350°, 350°]$, the variation of $\vec{q5}$ does not change the size of the collision-free area. Consequently $\vec{q5}$ can be specified to its maximum range: $q5 \in [-65°, 65°]$

Therefore, side conditions of $q4$ and $q5$ are defined as:

- $q4 \in [-350°, 350°]$
- $q5 \in [-65°, 65°]$

4.6 Definition of $q2$ and $q3$ ranges

The side conditions from above help to optimize the joint angle ranges $\vec{q2}$ and $\vec{q3}$. To solve the two-dimensional optimization problem (see equation 2), a configuration space of $q2$ and $q3$ can be generated based on the specified joint angle ranges $\vec{q4}$ and $\vec{q5}$ (see 3). The side condition

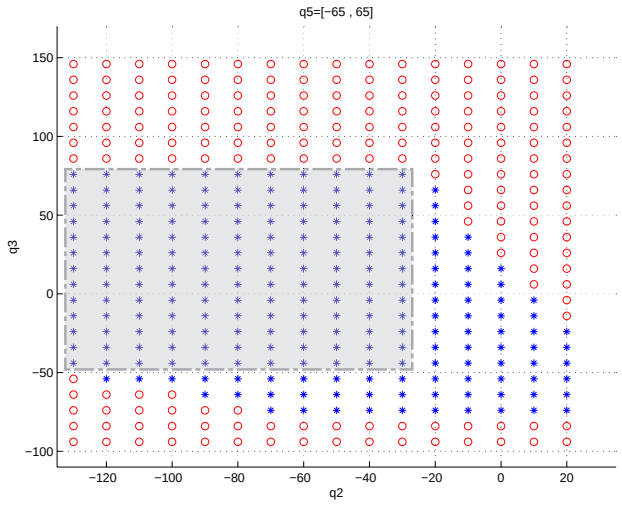

Figure 11. Definition of $\vec{q2}$ and $\vec{q3}$ according to case one

$q3_{min} > 0°$ (deduced in 4.4) is helpful to locate the ranges of $q2$ and $q3$ as it reduces the valid rectangular area within the configuration space.

Joint angles $q2 \geq -20°$ limit the joint angle $q3$ more and more. This results in a long but thin rectangle and smaller values of $A(\vec{q})$ (see figure 11). Therefore, joint angle $q2$ should be limited to a maximum value of $q2_{max} = -20°$. If $\vec{q2}$ is determined, the range $\vec{q3}$ with $q3_{min} > 0°$ can be optimized. Taking into account that $q4_{max} \geq 90°$ and $q4_{min} \leq -90°$ there are two essential possibilities of maximum $A(\vec{q})$:

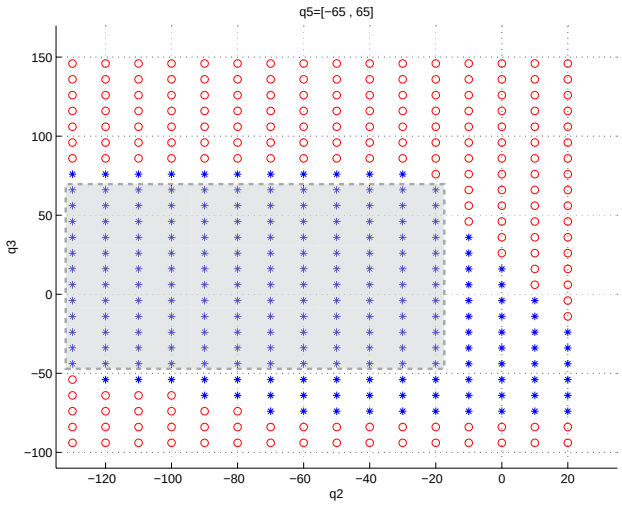

Figure 12. Definition of $\vec{q2}$ and $\vec{q3}$ according to case two

case 1) $q2 \in [-130°, -30°]$ and $q3 \in [-44°, 76°]$. $A_1(\vec{q}) = (-30 + 130) * (76 + 44) = 12000$. Figure 11 shows the corresponding configuration space; a sectional drawing of the collision-free area of the cartesian workspace is shown in figure 13.

case 2) $q2 \in [-130°, -20°]$ and $q3 \in [-44°, 66°]$. $A_2(\vec{q} = (-20 + 130) * (66 + 44) = 12100$. Figure 12 shows the corresponding configuration space; a sectional drawing of the collision-free area of the cartesian workspace is shown in figure 14.

Figure 13 and 14 show sectional drawings of the cartesian workspace at $q1 = 0$ with ranges $q4 \in [-350°, 350°]$, $q5 \in [-65°, 65°]$, $q6 \in [-350°, 350°]$ and corresponding values according to case one and two for ranges of $q2$ and $q3$ respectively. Each plus sign marks reachable positions

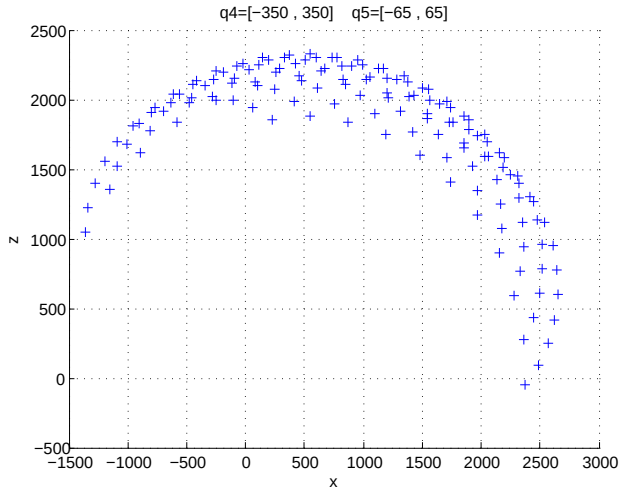

Figure 13. Sectional drawing at $q1 = 0$ of the collision-free workspace with ranges of case one

without collisions. The resolution of the collision check is $10°$. The difference in workspaces of both cases is depicted

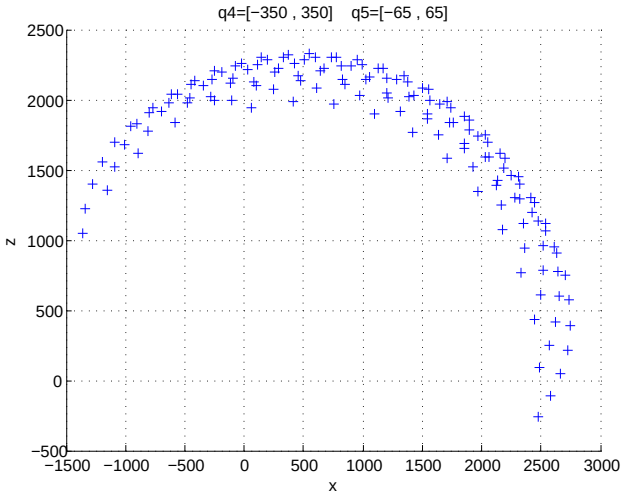

Figure 14. Sectional drawing at $q1 = 0$ of the collision-free workspace with ranges of case two

in figure 15. Green rectangles mark positions that can be reached only in the first case whereas blue plus signs mark positions that can be reached only in case two. A combination of both signs are positions that are reachable in both cases. This figure reveals that the definition of $\vec{q2}$ and $\vec{q3}$ according to case one is better suited for translational movements than those of case two.

4.7 Results

The optimization results in two essential possibilities of joint angle ranges:

- $q2 \in [-130°, -30°]$, $q3 \in [-44°, 76°]$, $q4 \in [-350°, 350°]$, $q5 \in [-65°, 65°]$, $q6 \in [-350°, 350°]$ and
- $q2 \in [-130°, -20°]$, $q3 \in [-44°, 66°]$, $q4 \in [-350°, 350°]$, $q5 \in [-65°, 65°]$, $q6 \in [-350°, 350°]$

Due to the redefinition of joint angle ranges, the workspace was significantly expanded in comparison to the workspace of the unmodified RoboCoaster. Figure 16 shows two different workspaces of reachable positions of a horizontal orientated passenger cabin with a resolution of $0,1m$. The workspace of the modified robot with optimized joint angle ranges provides a considerable larger spherical shell (figure 16 right) than the original RoboCoaster (figure 16 left) does. The red marker shows the longest translational distance in forward-backward direction, the blue marker in lateral direction.

The range of translational movements was increased by a factor of up to five. Instead of a translational distance of $0,1m$ in x-direction at a height of $z = 1m$, the optimized workspace for example provides a distance of $0,5m$.

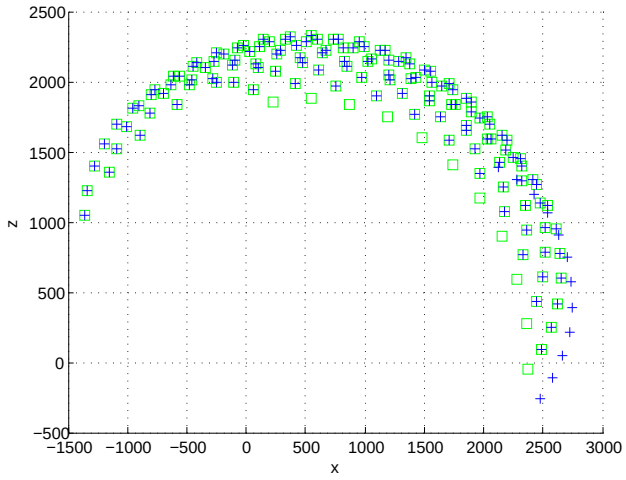

Figure 15. Difference of workspace with ranges of case one and two. Green rectangles mark position that can be reached only in the first case whereas blue plus signs mark positions that can be reached only in case two. A combination of both signs are positions that are reachable in both cases.

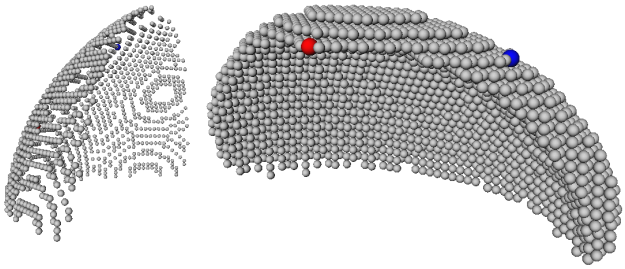

Figure 16. Reachable positions with a seat orientated constantly horizontal by the RoboCoaster (left) and by the robot with optimized joint angle ranges (right).

5 Conclusion

The optimization of joint angle limits is complicated as the limitation of one joint angle has a great effect on other joint angle limits.

Due to the presented approach, the multi-dimensional optimization problem was separated in several subproblems. Based on application specific constraints that the simulator must fulfill, side conditions of joint angles $q4, q5$ and $q6$ were derived. Joint angle $q1$ had no effect on this investigation.

These side conditions enabled to reduce the six-dimensional to a two-dimensional optimization problem. Based on configuration spaces of $q2$ and $q3$ the collision-free cartesian workspace was investigated by a variation of joint angle ranges of $q2$ and $q3$.

Both resulting configurations of hardware joint limits comply with the requirements of a driving and flight simulator. However, the operator must choose the combination

of joint angle limits that fit best for his application.

As the determination of joint angle ranges and joint angle limits is dependent on the dimensions of the passenger cabin and the application, a general solution cannot be generated.

Acknowledgement

This work was partially funded by the Kuka Roboter GmbH, Augsburg, Germany.

References

[1] D. Stewart, A platform with six degree of freedom, *Proc. of the Institution of Mechanical Engineering*, vol. 180, 1965, 371-386.

[2] L. Pollini; M. Innocenti, Study of a Novel Motion Platform for Flight Simulators using an Anthropomorphic Robot, *Proc. of AIAA Modeling and Simulation Technologies Conference and Exhibit*, Keystone, USA, 2006.

[3] T. Bellmann, An Innovative Driving Simulator: Robocoaster, *Proc. of FISITA, World Automotive Congress*, Munich, Germany, 2008.

[4] http://www.kuka-entertainment.com/en/products/robocoaster/start.htm

[5] http://www.kuka-robotics.com/germany/en/products/industrial_robots/heavy/kr500_2/start.htm

[6] J. Heindl, M. Otter, H. Hirschmueller, The Robocoaster as Simulation Platform: Experiences from the First Authentic Mars Flight Simulation , *Proc. of the first Motion Simulator Conference*, Braunschweig, Germany, 2005.

[7] P. Grant, L. Reid, Motion Washout Filter Tuning: Rules and Requirements, *Journal of Aircraft*, 34(2), 145-151, 1997.

[8] M. Bruenger-Koch, S. Briest, M. Vollrath, Do you feel the difference? A motion assessment study, *Proc. of DSC Driving Simulation Conference*, Tsukuba, Japan, 2006.

[9] T. Bellmann, M. Otter, J. Heindl, Real-Time Path Planning for an interactive and industrial robot-based Motion Simulator, *Proc. of 2nd Motion Simulator Conference*, Tsukuba, Braunschweig, Germany, 2007.

[10] H. Teufel, H.G. Nusseck, K.A. Beykirch, J.S. Butler, M. Kerger, H.H. Buelthoff, MPI Motion Simulator: Development and Analysis of a Novel Motion Simulator, *Proc. of AIAA Modeling and Simulation Technologies Conference and Exhibit*, Hilton Head, USA, 2007.

[11] J. Schroeder, Helicopter Flight Simulation Motion Platform Requirements, *NASA Technical Report*, USA, 1999.